Measurements of Temperature and Flow Fields with Sub-Millimeter Spatial Resolution Using Two-Color Laser Induced Fluorescence (LIF) and Micro-Particle Image Velocimetry (PIV)

Hyun Jung Kim*

Division of Mechanical Engineering, Ajou University,
San 5 Wonchon-Dong, Yeongtong-Gu, Suwon 443-749, Korea

Comprehensive measurements for velocity and temperature fields have been conducted. A Micro PIV 2-color LIF system have been setup to measure the buoyancy driven fields in a 1-mm heated channel with low Grashof-Prandtl numbers [$86 < Gr_w Pr < 301$] Fluorescence microscopy is combined with an MPIV system to obtain enough intensity images and clear pictures from nano-scale fluorescence particles The spatial resolution of the Micro PIV system is 75 μm by 67 μm and error due to Brownian motion is estimated 1.05% Temperature measurements have achieved the 4 7 μm spatial resolution with relatively large data uncertainties the present experiment. The measurement uncertainties have been decreased down to less than ± 1.0 C° when measurement resolution is equivalent to 76 μm Measured velocity and temperature fields will be compared with numerical results to examine the feasibility of development as a diagnostic technique

Key Words : Fluorescence, Laser, Micro PIV, Temperature Measurement

1. Introduction

Recently, micro-electromechanical system (MEMS) is being developed to respond to an increasing demand of industry and research problems Meanwhile, micro-channel flows, having characteristic dimensions in the range of 1-1000 μm are frequently occurring in a wide range of MEMS devices. Being different from macro-scale devices, micro-fluidic systems prefer to use different pumping mechanisms instead of pressure pumping In pressure driven systems of the micro-fluidics, the frictional forces at the wall result in radical velocity gradients throughout the micro-channel. As a result, fluid velocity is greatest in the middle of the micro-channel and a substantial pressure drop along micro-channel occurs In other words, it has limitations in applying it to MEMS devices Therefore, MEMS devices are frequently using electro-osmosis, thermally-driven forces, thermo-capillary forces and so on as alternative driving forces

Although some researchers (Kim et al 2001, Cummings et al 1999) measured the electro-osmosis and pressure driven flow in a micro-channel, the measurement of velocity fields in thermally-driven flows have not been reported Since the dimension of micro-channel has length scale on the order 1-1000 μ, the intrusive technique such as a hot wire can not be used In recent years, Particle Image Velocimetry (PIV) has been developed and modified to be applied to micro-scale

Among the available means of temperature measurement probes, there is no question regard-

* **E-mail** hyunkim@ajou ac kr
TEL +82-31-219-2340, **FAX** +82-31-213-7108
Division of Mechanical Engineering, Ajou University, San 5 Wonchon-Dong, Yeongtong-Gu, Suwon 443-749, Korea (Manuscript **Received** July 16, 2004, **Revised** December 31, 2004)

ing the extensiveness and rigorousness of thermocouple (TC) probes for a wide range of heat transfer applications A carefully calibrated TC probe is capable of measuring temperatures with better than ±0 1 K precision (Eckert and Goldstein, 1970) Two primary limitations of TC probes, however, are their relatively large spatial resolution, on the order of a few hundred microns at the smallest, and their physical intrusiveness in the flow These limitations diminish the possibility of using TC probes for micro-scale heat transfer applications In addition, their point measurement nature makes full-field temperature mapping very cumbersome as a large number of probes must be placed and monitored simultaneously

The thermo-chromic liquid crystals (TLC) technique is based on the temperature dependence of their optical properties in a predictable and repeatable manner (Dabiri and Gharib, 1990, 1991). When TLC is illuminated, TLC selectively reflects light at a visible wave length characterized by the local temperature This relationship of color to temperature has allowed researchers to quantitatively map temperature distributions (Richard, 1998, Pehl, 2000).

A major shortcoming in using TLC is that one has to calibrate each point of the test field to compensate for the influence of the illuminating light variations (Sabatino, 2000) Since the color change of the TLC may also depend on its location in the test field, the temperature calibration has to be tediously repeated at each different test section. The color bias, occurring from the wall reflection and scattering, is another obstacle in applying the TLC technique to full-field mapping Another major drawback of the TLC technique for considering micro-scale field-of-view measurements is the relatively large size of microencapsulated TLC beads, typically on the order of 10 μm or larger

Sakakibara and Adrian (1997, 1999) recently proposed an innovative two-color LIF technique where they used a second temperature-insensitive fluorescence dye as a reference to compensate for the variation of incident light and the spatial imaging nonuniformity The ratio of the two fluorescences dyes intensity provides a formidable correlation with temperature that does not depend on the laser illumination intensity variation and is free from the possible bias occurring from background noise They applied this ratiometric LIF technique to measure a thermal convection field above a heated horizontal surface of 40 mm square in dimension, showing a calibration uncertainties of ±1 5 K over 25 K temperature range

In this paper, comprehensive measurements of velocity and temperature fields will be conducted The present work uses a similar ratiometric LIF technique to quantitatively examine the measurement accuracy, in conjunction with its spatial resolution, for the feasibility as a microscale temperature field-mapping tool. A 1 0 mm wide cuvette is heated differentially on opposite vertical sides so as to generate a natural convection thermal field, with relatively lower $Gr_wPr < 300$, and the resulting steady temperature field has been measured by the ratiometric LIF technique Also, a micro PIV system will be set up to measure thermal driven velocity fields in the same heated channel Fluorescence microscopy will be combined with an MPIV system to get enough intensity images and clear pictures from nano-scale fluorescence particles The measurement accuracy is assessed by comparing the measured temperature and velocity field with computational predictions, which can be considered accurate for the near-conduction regime of low Gr_wPr, and the measurement uncertainties are determined for different spatial resolutions ranging from 4 2 μm to 76 μm

2. Micro PIV Systems

The micro PIV experimental apparatus uses 500 nm fluorescence seeding particles which have an excitation peak at 490 nm and an emission peak at 515 nm These absorption and emission bandwidths partially overlap each other To detect fluorescence signals more exclusively, the fluorescence detection band must be separated from the emission and absorption bandwidths, to the extent possible The selection is made for the

long pass filter (Edmund Industrial Optics) that transmits wavelengths longer than 530 nm This filtering process passes a pure fluorescence image of seeding particles without accepting scattering of the background illumination of the excitation light

In addition, Mie scattering intensity decreases as the diameter of the seeding particles decreases while the fluorescence signal is much stronger than the Mie scattering for sub-micron seeding particles Therefore, using fluorescence seeding particles is almost essential to get an high image intensity for micro PIV The interline transfer 640×480 CCD camera (Sony XC-75) with 5× objective lens (Mitutoyo) was used for recording particle images The sensing area of the CCD chip has a 6 4 mm×4 8 mm dimensions and the size of each pixel is approximately 8 4×9 8 μm A thin laser sheet is constructed from a 50 mW argon-ion laser using a combination of one concave and one spherical lens

2.1 Lasers and optics

An Argon-ion laser can be commonly used for micro-scale experiments The reason is that a continuous wave laser such as the Argon-ion laser is sufficient for slow flows that usually happen in microfluidic applications Another reason is that fluorescence particles of which the absorption wave length band ranges around Argon-ion laser emission wave length are easy to be obtained commercially

In micro PIV, measurement domain in the out of plane can not be defined by thickness of laser sheet because it is hardly possible to get the order of micron thickness of laser sheet in micro system with the severe restriction on spacing Therefore, depth of field of the microscope is an important factor Inoue and Spring (1997) reported the formulation for depth of field, considering diffraction and geometric affects as

$$\delta z=\frac{n\lambda}{NA^2}+\frac{ne}{M\cdot NA} \tag{1}$$

where the index of refraction of medium is $n=1\ 0$, the wavelength of illuminating light is $\lambda=488$ nm, the numerical aperture is $NA=0\ 14$, the magnification is $M=5$ and pixel size is $e\approx 9$ μm. Thus, the depth of field in the current experiment is estimated to $\delta z=14\ 29$ μm

2.2 Measurement error from Brownian motion

Brownian motion must be considered when submicron particles are used Brownian motion is known to be the thermal motion of a particle in a fluid This motion results from collisions between fluid molecules and the suspended micro-scale particles Santiago et al (1998) demonstrated the effect of Brownian motion on microfluidics measurement where the Brownian motion error is derived as

$$\varepsilon_B=\frac{1}{u}\sqrt{\frac{2D}{\Delta t}} \tag{2}$$

where u is the characteristic velocity, Δt is the measurement time interval and D is the diffusion coefficient

For a single PIV realization, ε_B is calculated to be 7 4% in that u is 10 μm/s, T is 20℃ and Δt is 1/30s This error means the ratio of Brownian motion to the measured flow velocity

Because the Brownian motion error is considered having the same effect in all directions statistically, the error by the Brownian diffusion can be reduced by use of averaging technique (Santiago et al, 1998) If one assumes that each particle has equal influence on average velocity vector in the interrogation window, can be reduced by averaging over several particle images (at least 5 pairs in the current experiment) and ensemble averaging over several realizations (at least 10 realizations) Therefore, the Brownian motion error is reduced to $\varepsilon_F=\frac{\varepsilon_B}{\sqrt{50}}=1\ 05\%$

3. Two-Color LIF Systems

3.1 Principles of fluorescence and ratiometric LIF techniques

Fluorescent intensity is proportional to the incident light intensity and quantum efficiency As the temperature increases, the quenching effect increases and the quantum efficiency decreases. The temperature dependence of quantum efficiency

is usually small in most fluorescent molecules. However, for some fluorescence dyes such as Rhodamine-B, the temperature dependence of quantum efficiency is noticeably high, about 2%/K. Therefore, if the incident light intensity is constant and homogeneous with temperature sensitive fluorescence dye, the correlation between temperature and fluorescence intensity can be expected to be obtained. But incident light is likely to be inhomogeneous, spatially as well as temporally, because of the laser beam or sheet divergence, scattering by small particles in the beam path, and time-dependent lasing efficiency (Sakakibara and Adrain, 1999). In order to compensate the measurement bias caused by the incident light variation, Rhodamine-110 is used for the reference dye whose photo-thermal sensitivity is known to be less than 0.05%/K.

For the mixture of Rhodamine-B and Rhodamine-110, the intensity ratio of the two fluorescence emissions can be directly given from Eq. (3) as:

$$\frac{F_{rhb}}{F_{rh110}} = \frac{I_{0rhb}\varepsilon_{rhb}[c]_{rhb}Q_{rhb}}{I_{0rh110}\varepsilon_{rh110}[c]_{rh110}Q_{rh110}} \qquad (3)$$

where molar absorptivity is nearly independent of temperature (Andrews, 1986), and the ratio of the absorption spectral intensity, I_{0rhb}/I_{0rh110}, is invariant when a single illumination source is used for both dyes. In addition, if the concentration ratio, $[c]_{rhb}/[c]_{rh110}$, remains unchanged, the fluorescence intensity ratio, F_{rhb}/F_{rh110}, is solely dependent on the quantum efficiency ratio of the two dyes, Q_{rhb}/Q_{rh110}. Since the ratio of the quantum efficiency depends on temperature, the resulting intensity ratio of Eq. (3) can now be considered solely dependent on temperature.

3.2 Calibration process

Figure 1 shows the semi-quantitative absorption and emission spectra of Rhodamine-B and Rhodamine-110. The wavelength of maximum absorption and emission for Rhodamine-110 (Molecular Probes) is at 496 nm and 520 nm, respectively. Rhodamine-B (Baker, Inc.) has an absorption band peaked at 554 nm and an emission band peaked at 575 nm. These four bandwidths partially overlap each other. To minimize signal errors due to the cross-talk, the fluorescence detection band for each dye must be segregated from the other emission and absorption bandwidths, to the extent possible. For the Rhodamine-B detection bands, selection is made for the long pass filter (Edmund Industrial Optics) that transmits wavelengths only longer than 560 nm. This filter has a mere 0.001% transmission of shorter wavelengths than 560 nm. Since Rhodamine-110 emission band is placed between the Rh-110 absorption band and Rh-B absorption band, a narrow band-pass filter (505 nm~515 nm) is selected to effectively separate the Rh-110 emissions. The spectral band of an argon-ion laser, peaked at 488 nm (blue), is used to excite both dyes.

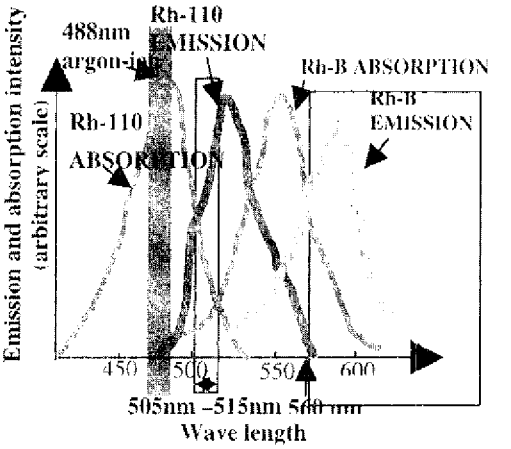

Fig. 1 Absorption and fluorescence spectra of Rhodmine-110 and Rhodamine-B

The correlation between fluorescence intensity and temperature is necessary to use a LIF technique for temperature measurement. To obtain a correlation between the measured fluorescence intensity and the water temperature, an elaborate calibration system is devised using a constant thermobath as schematically illustrated in Fig. 2. The thermobath circulates constant-temperature water through a 15 cm cubic chamber which is made of 0.6 cm thick plexiglass walls covered with ample insulation material to minimize the ambient thermal effect. A 3.5 cm square glass window has been installed on the front wall for optical access. The test cuvette (Cole Parmer)

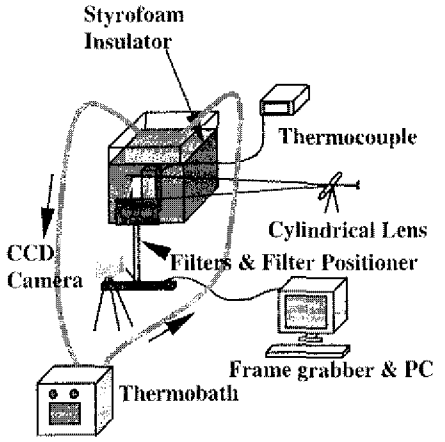

Fig. 2 Schematic layout of the calibration setup for two-color LIF technique

contains a 6 mg/liter concentration of Rh-B and 1 mg/liter concentration of Rh-110, and the cuvette is placed in the midst of the cubic chamber. The water temperature surrounding the cuvette is monitored using a thermocouple probe placed in the chamber.

A Sony XC-75 CCD camera with 5×objective lens records fluorescence images from Rh-B and Rh-110 by alternating the two filters and an approximately 1.5 mm by 1.0 mm field-of-view is used for calibration, corresponding to 320 by 240 pixel dimensions. A thin laser sheet is constructed from the same lens combination and Ar-ion laser with above micro PIV system. Captured images from the CCD camera are digitized for successive gray-level analysis. Although 2-color LIF system uses the similar optical system to micro PIV, the diameter of fluorescence dyes is much smaller that one of fluorescence seeding particle. The diameter of fluorescence molecule dyes is much smaller than 10 nm. So each fluorescence molecule can't be detected by pixel of CCD camera. One pixel may present the average intensity of above 100, 000 dye molecules. Because fluorescence dyes are resolved homogeneously into water, the number of dye molecules in each pixel is considered consistent. Also due to the random motion of Brownian motion, the average intensity of each pixel is expected not to be influenced statistically. The key to success in calibration is to ensure the repeatability of the calibration curves and the persistency in dye concentrations for each calibration process. Due to chemical and photochemical decomposition, the intensity of fluorescence dye may degrade during excitation and emission transitions (Sakakibara and Adrian 1997). Therefore, a fresh mixture of fluorescence dyes has to be used for each run of the calibration experiment.

In order to ensure the repeatability, the calibration was repeated on three different test days for the same temperature range from 16℃ to 40℃. Figure 3 presents the same calibration data in terms of the intensity ratio of Rh-B over Rh-110. Each symbol represents a pixel-averaged intensity for the entire 1.5 mm by 1.0 mm field-of-view (320 by 240 pixels). The day-to-day variations are smaller than 3%. It is important that the mixture of dye is contained in the closed system to maintain the given dye concentration. Otherwise, the different calibration curve is obtained due to the change of dye concentration as the day of calibration change. The average of the three sets of calibration data, shown by the solid curve, can now be used as a resulting calibration curve for temperature measurement. The day-to-day variations of the intensity ratio show a decrease with increasing temperatures.

To examine the effect of spatial resolution on the intensity variations, statistical analysis of the calibration data has been conducted as the interrogation cell size is increased from a single pixel

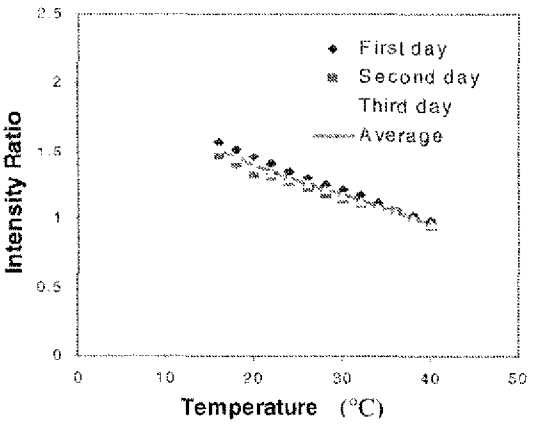

Fig. 3 Temperature dependence of the ratiometric fluorescence intensities of RhB and Rh110

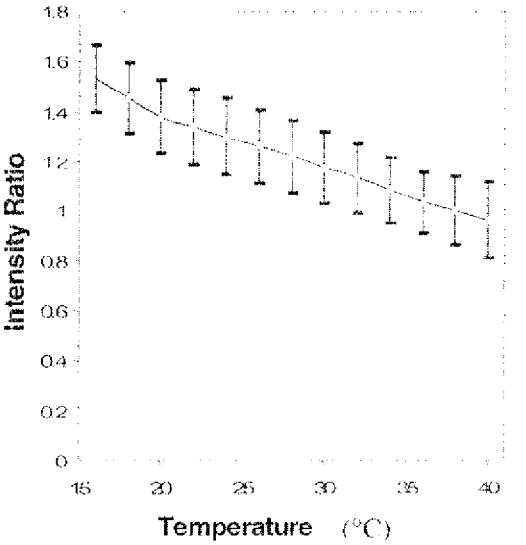

(a) Interrogation window dimension of 1 by 1 pixel (4.7 μm×4.2 μm)

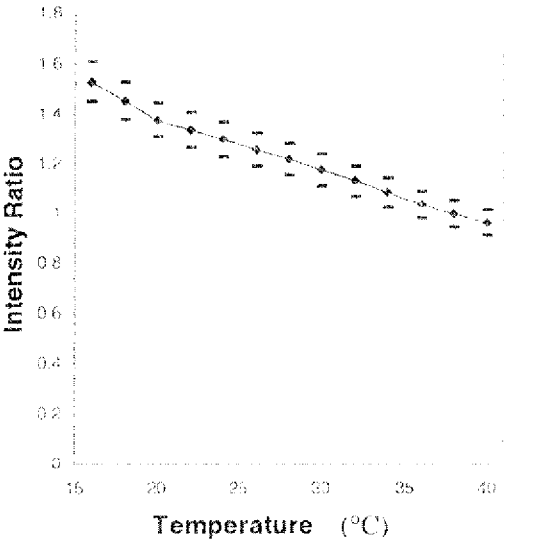

(b) Interrogation window dimension of 10 by 10 pixels (47 μm×42 μm)

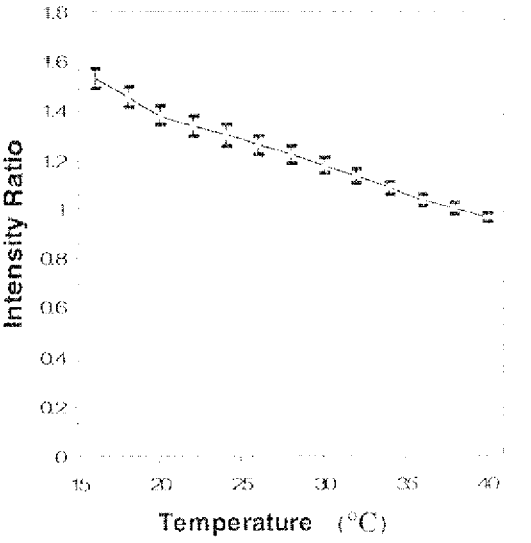

(c) Interrogation window dimension of 64 by 48 pixels (300 μm×200 μm)

Fig. 4 Deviation of intensity Ratio vs. Temperature

to the whole field-of-view. Figures 4(a), (b) and (c) show the average and standard variation of the intensity ratio as functions of temperature for the selected three different interrogating window dimensions of 1 by 1 pixels (4.7 μm×4.2 μm), 10 by 10 pixels (47 μm×42 μm), and 64 by 48 pixels (300 μm×200 μm), respectively. The corresponding pixel-to-pixel temperature variation is estimated as ±5.64℃ for 1 by 1 pixel, approximately ±3.0℃ for 10 by 10 pixels, 2.0℃ for 32 by 24 pixels, and ±1.5℃ for 64 by 48 pixels with 300 μm×200 μm spatial resolution. While the standard variations of intensity ratios, for a given temperature, persistently increase with decreasing window dimensions, note that the average intensity ratio remains constant for a given temperature regardless of the spatial resolution.

Table 1 Spatial-resolution dependency of the calibration uncertainties of two-color LIF technique

Interrogation window Dimension (pixels)	Spatial Resolution (μm)	Intensity Ratio Deviation	Temperature Deviation
1 by 1	4.7×4.2	±0.143	±5.635
10 by 10	47×42	±0.056	±2.964
32 by 24	150×100	±0.043	±1.967
64 by 48	300×200	±0.033	±1.496
128 by 96	600×400	±0.022	±1.006
256 by 192	1200×800	±0.009	±1.496
320 by 240	1500×1000	±0.000	±0.000

Table 1 summarizes the results where the standard deviation is calculated for each calibration temperature with 95% confidence interval for a given interrogation cell size and listed deviations are the average values for the tested temperature range from 16 to 40℃. The intensity ratio deviations are presented in the third column and the corresponding temperature deviations are shown in the fourth column. As the interrogating window dimension increases, the variation of intensity ratio decreases and diminishes ultimately to zero when the whole field-of-view is considered as a single interrogation window.

Once the calibration data is obtained, a test section can be positioned instead of cubic chamber for the temperature measurement.

4. Experiment

A 1 mm wide, 10 mm deep, and 45 mm long cuvette (Nova Biotech Inc.) is used for the 1 mm channel configuration.

To establish a thermal field inside the 1 mm cuvette, an elaborate system is devised using constant thermobaths as schematically illustrated in Fig. 5.

The constant-temperature water wall condition was provided by two separate thermal baths circulating hot and cold water through copper pipelines. The copper pipelines are attached to side walls. Hot water flows through the right wall pipe line and cool water flows through the left one to induce the thermally buoyancy driven flow in the channel. To ensure a more homogeneous

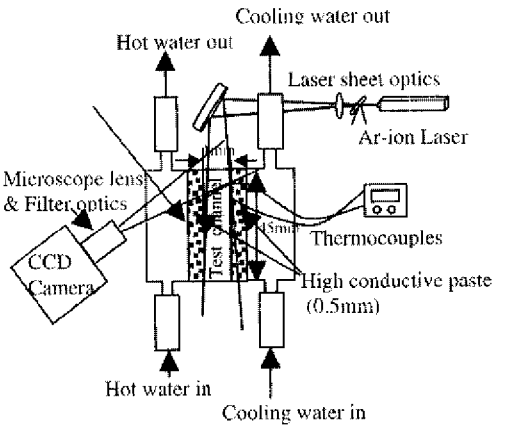

Fig. 5 Experimental Apparatus for MPIV and 2-color LIF

thermal contact, the copper pipelines and cuvette are bonded by a high thermal-conductivity paste. A K-type thermocouple probe is attached to both sides of the channel wall using thermal-conductivity epoxy. The temperature is monitored as a feedback signal to ensure if both walls are heated and cooled at specified temperatures. Typically it takes up to 30 minutes for both walls to reach the required steady state temperature conditions within ±0.5 C°.

Captured images from the identical imaging system in previous chapter are digitized for PIV and 2-color LIF analysis at 30 frame per second. In Fig. 5, the test channel for micro PIV system contains a mixture of 500 nm fluorescence particles and water. The test channel for 2-color LIF system contains a mixture of fluorescence dyes and water at a typical concentration of 6 mg/liter for Rh-B and 1-mg/liter for Rh-110. The

measured imaging area is approximately 1.5 mm by 1.0 mm. As explained previously, appropriate filters are positioned in front of CCD camera in both systems.

Numerical predictions for temperature and velocity fields are also carried out for the same parametric condition as the experiment.

Two-dimensional steady state momentum and energy equations are solved with imposed flow and thermal conditions as used in the experiments using standard Finite Volume Method (FVM (Patankar, 1980). The v-momentum equation includes the buoyancy term using the Boussinesq approximation to model the density gradient driven flow (Chuichi, 1994). The SIMPLE(Semi-Implicit Method for Pressure-Linked Equation) algorithm is adopted to obtain the pressure field. The grid dimension was set to 19×380 for the entire calculations. Around 3,000 iterations were required to reach an acceptable convergence that usually takes approximately 5 CPU minutes on the Pentium 4 1.2 GHz PC platform. The relaxation factor for all the variables was set to be 0.5.

Measured velocity and temperature fields are compared with numerical results to examine the accuracy of development to a diagnostic technique.

5. Results and discussion

PIV measurements are conducted for two representative of the top region of the 1-mm vertical channel. Four different wall temperature differentials, 16-20℃, 18-24℃, 20-30℃ and 23-37℃ are considered with their corresponding Rayleigh number, Gr_wPr=86, 129, 215 and 301, respectively. The Rayleigh numbers are well below the critical value of 10^9, all test conditions are under laminar flows (Incropera, 2002).

Figure 6 shows flow fields for the top region of channel. An interrogation window of 32×32 pixels was taken, with a 50% overlap rate using direct cross correlation and velocity fields from 150 images were averaged. This corresponds to a vector spatial resolution of 75 by 67 μm. The left column shows the calculated flow results and the right column shows the measured ones. Fairly

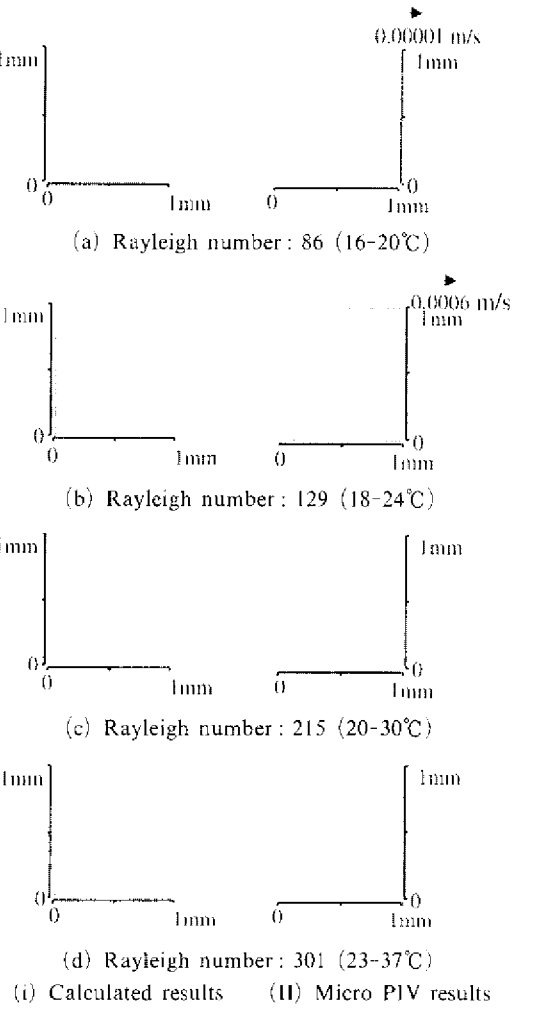

Fig. 6 Velocity field for the top region of a heated channel

good agreements are observed between numerical and the PIV results. The magnitudes of velocity increase as the temperature difference increases while the qualitative flow patterns remain unchanged for all four conditions. The heated liquid rises up along the left wall and circulates against the top wall, and then descends along the right wall.

For a quantitative comparison between calculated and measured velocity, velocities on the horizontal line below 0.15 mm and 0.65 mm from the top of the channel is plotted in Fig. 7 for 20℃ and 30℃ temperature difference conditions. PIV velocity has a good agreement with calculated velocity. As we identified it for below 0.15 mm

from the top in Fig. 7, U-velocity has a maximum value in a center of the horizontal line. U-velocity goes to a zero value near walls due to viscous from the wall. V-velocity has positive values in the right side and negative values in the left side, indicating the clockwise-direction flow circulation. For below 0.85 mm from the top, positive V-velocity indicates rising flow from the heated wall and negative V-velocity shows the returning flow, making the clockwise-direction flow circulation. The slight deviation between calculated and measured velocity is considered to result from the existence of three dimensional flows. Although the particles should be circulated on the 2-dimensional focal plane, there might exist small amount of 3-dimensional flow in practical which caused to underestimate the displacement of particles from the cross correlation process.

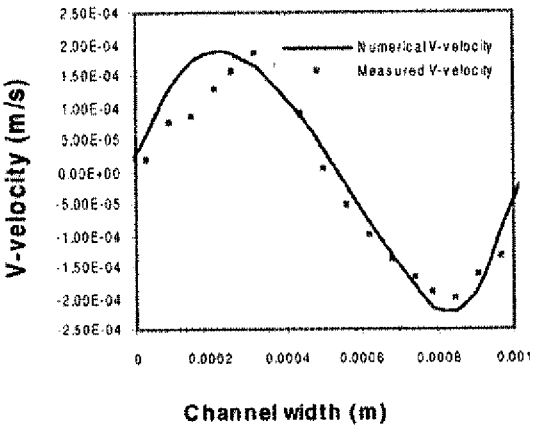

(a) V-velocity for below 015 mm from the top

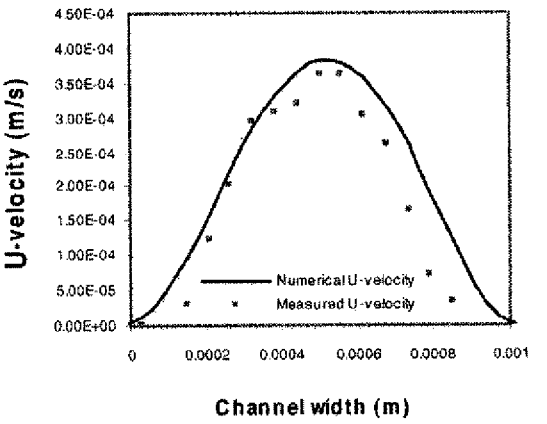

(b) U-velocity for below 015 mm from the top

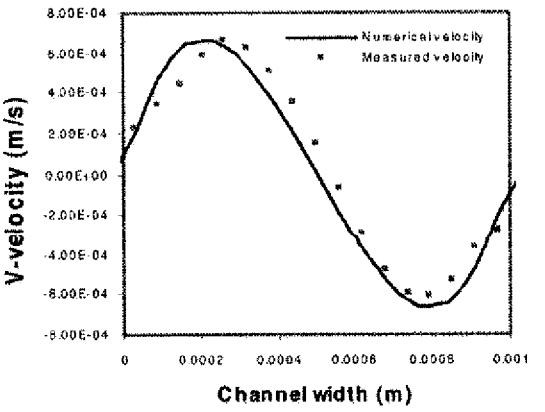

(c) V-velocity for below 085 mm from the top

Fig. 7 The comparison of numerical and micro PIV velocity values below 0.15 mm and 0.85 mm from the top ($Gr_w=Pr=215$, $T_L=20℃$ and $T_H=30℃$)

Figure 8 show the numerical and 2-color LIF experimental results for temperature field of the top region of the 1 mm channel. Also, the left and

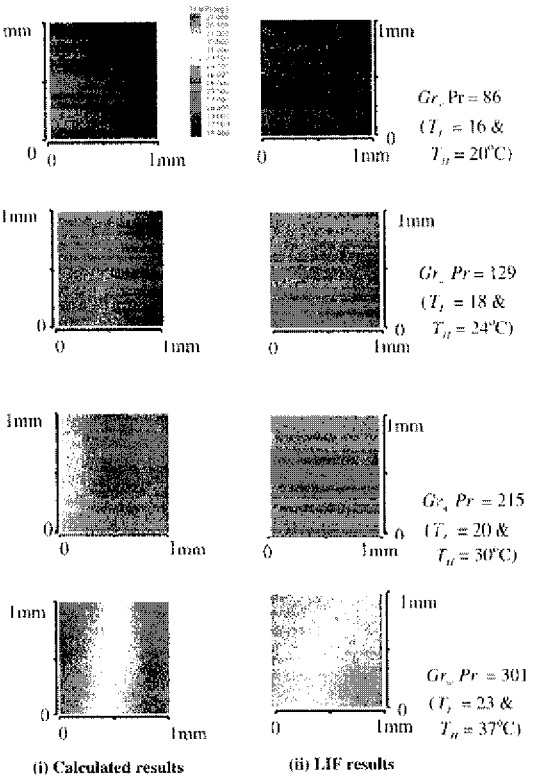

(i) Calculated results (ii) LIF results

Fig. 8 Temperature field for the top region of a heated channel

right column shows the calculated and the measured results, respectively. The temperature contours for 16-20℃ and 18-24℃ cases show nearly vertically stratified profiles. The reason is that the very slow flow circulation due to the small Raleigh numbers is not sufficient to deform the temperature contours. As such low Rayleigh numbers, there exists little free-convection current and the heat transfer occurs mainly by conduction across the fluid layer (McGregor, 1969). The

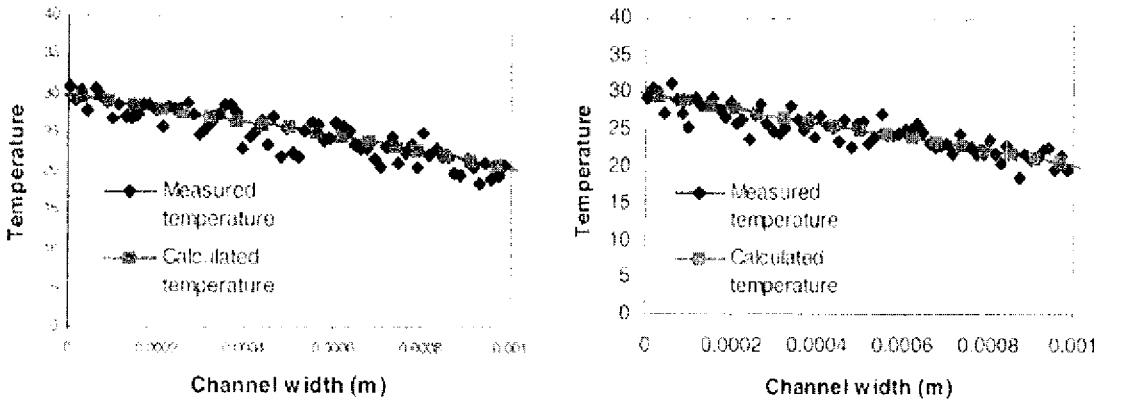

(a) Spatial resolution : 19 μm (h) by 19 μm (v)

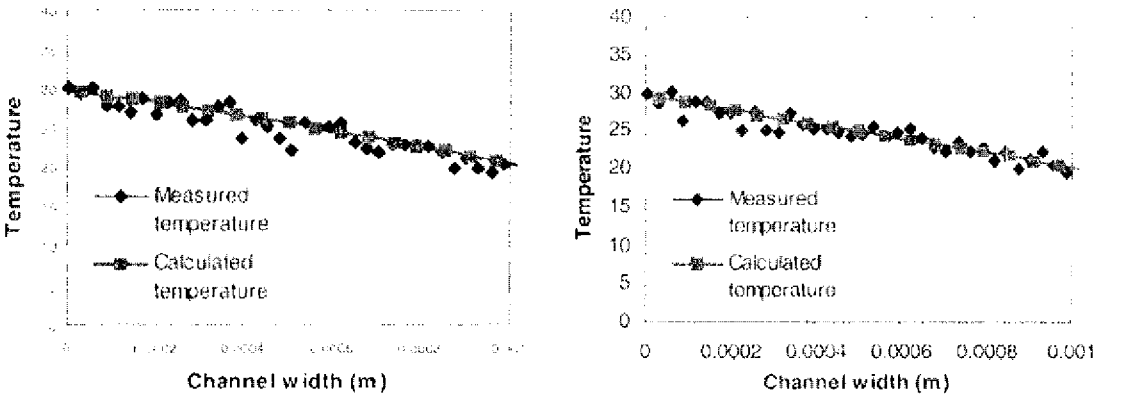

(b) Spatial resolution : 38 μm (h) by 38 μm (v)

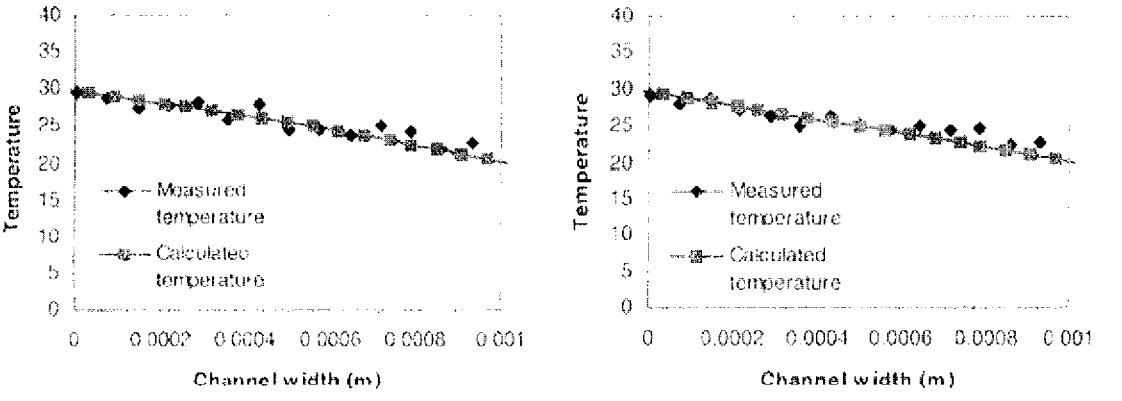

(c) Spatial resolution : 76 μm (h) by 76 μm (v)

(A) 0.15 mm below the top (B) 0.85 mm below the top

Fig. 9 The comparison of numerical and 2-color LIF temperature values below 0.15 mm and 0.85 mm from the top (Gr_wPr=215, T_L=20℃ and T_H=30℃)

horizontal variation in temperature should remain largely linear when the flow remains in the conduction regime of $Gr_wPr \leq 10^3$ as long as $h/w \geq 10$ However, with increasing the Rayleigh number, the temperature contour starts deforming as seen for cases of 20-30℃ and 23-37℃ The clockwise circulation more aggressively moves hotter fluid from the left wall to the cooler right wall region Therefore, the temperature contour deforms to the right side reflecting the stronger thermal convection This fact can also be identified in PIV results which show that the magnitudes of velocity increase as the temperature difference increases. Figure 9 shows local and more quantitative comparisons between the measured and calculated temperature profiles at 0 15 mm and 0 85 mm below the top, for a representative case of $Gr_wPr=215$ To examine the measurement uncertainties as a function of the spatial measurement resolution, the original pixel-by-pixel data are combined to 4×4, 8×8, and 16×16 - pixeled interrogation cells, corresponding to the spatial resolution of 19 μm (H) by 19 μm (V), 38 μm by 38 μm, and 76 μm by 76 μm, respectively

The data fluctuations should decrease with increasing number of the spatial samplings and the uncertainties are proportional to $1/\sqrt{N}$, for the case of multiple (N) samplings with N approaching to infinity The root-mean-square (r m s) fluctuations of the measured temperature data, from the calculated predictions, show persistent reduction from over 2℃ to below 1℃, with increasing spatial resolution from 19 μm square to 76 μm square.

6. Conclusions

Micro Particle Image Velocimetry (PIV) and Two-color Laser Induced Fluorescence (LIF) technique has been developed and examined for the comprehensive measurements for velocity and temperature fields The measurements have been accomplished for buoyancy driven velocity and temperature fields in a 1 mm heated channel The spatial resolution of the Micro PIV system is 75 μm by 67 μm and the error due to Brownian motion is estimated 1 05% In 2-color LIF system, detection of the fluorescence intensity ratio of the temperature-sensitive Rh-B to the temperature-insensitive Rh-110 enables temperature measurements that are free from the background noise occurring primarily from the nonuniformity of incident laser sheet It is shown that the intensity ration of fluorescence follow the thermal-driven flow faithfully in the 1 mm channel The r m.s fluctuations of the measured temperature from the computational predictions show persistent decrease from 2 3℃ for 19 μm spatial measurement resolution to 0 92℃ for 76 μm resolution Measured velocity and temperature fields have fairly good agreement with numerical results, showing the feasibility of development as a diagnostic technique

Acknowledgments

This material is based on the work supported by the grant of Ajou University and the National Research Laboratory (Thermo-mechanical Properties Measurement Laboratory), established by Korea Institute Science and Technology Evaluation and Planning

References

Andrews, D L , 1986, *Lasers in Chemistry*, Springer-Verlag, Berlin

Chuichi, A , 1994, *Computational Fluid Dynamics for Engineering*, University of Tokyo Press, Tokyo

Cummings, E B , Griffiths, S. K. and Nilson, R H , 1999, "Irrotationality of Uniform Electroosmosis," Proceeding of SPIE Microfluidics Devices and Systems II, pp 180～189

Dabiri, D and Gharib, M., 1990, "Digital Particle Image Thermometry and its Application to a Heated Vortex Ring," *Proc. Fluid Measurement and Instrumentation Forum*, ASME FED-95, pp 27～34

Dabiri, D and Gharib, M , 1991, "Digital Particle Image Thermometry the Method and Implementation," *Experiments in Fluids*, Vol 11, pp 77～86

Eckert, E. R. and Goldstein, R. J, 1970, *Measurements in Heat Transfer*, McGraw-Hill, New York

Inoue, S and Spring, K R, 1997, *Video Microscopy, 2nd ed*, Plenum Press, Oxford.

Kim, M J, Kim, H J and Kihm, K D, 2001, "Micro-Scale PIV for Electroosmotic Flow Measurement," *Proc PSFVIP-3*, F3112, March 18-21, Maui, HI.

Incropera, F P and Dewitt, D P, 2002, *Fundamentals of Heat and Mass Transfer*, John Wiley & Sons, New York, pp 539~543

Mcgregor, R K, Emery, A. P, 1969, "Free Convection through Vertical Plane Layers Moderate and High Prandtl Number Fluids," Journal of Heat Transfer, Vol 91, pp 391~396

Patankar, S V, 1980, Numerical Heat Transfer and Fluid Flow, Taylor & Francis, New York

Pehl, M., Werner, F and Delgado, F A., 2000, "First Visualization of Temperature Fields in Liquids at High Pressure Using Thermochromic Liquid Crystals," *Experiments in Fluids*, Vol 29, pp. 302~304

Sabatino, D R, Praisner, T, J, Smith, C R., 2000, "A High-Accuracy Calibration Technique for Thermochromic Liquid Crystal Temperature Measurements," *Experiments in Fluids*, Vol 28, pp 497~505.

Richards, C. D and Richards, R F, 1998, "Transient Temperature Measurements in a Convectively Cooled Droplet," *Experiments in Fluids*, Vol. 25, pp 392~400

Sakakibara, J and Adrian, R J., 1997, "Measurement of Whole Field Temperature Using Two-Color LIF," *Journal of Visualization Society*, Japan, Vol 17, pp 333~336

Sakakibara, J and Adrian, R J, 1999, "Whole Field Measurement of Temperature in Eater Using Two-Color Laser Induced Fluorescence," *Experiments in Fluids*, Vol 26, pp 7~15

Santiago, J G, Wereley, S T., Meihart, C D, Beebe, D J and Adrian, R J, 1998, "A Particle Image Velocimetry System Microfluidics," *Experiments in Fluids*, Vol. 25, pp 316~319